A SIMPLE METHOD FOR POWER LOSS ESTIMATION IN PWM INVERTER-FED MOTORS

Ş.G. Roşu*, C. Rădoi*, M. Teodorescu*, P. Guglielmi, I. R. Bojoi**, M. Pastorelli****

*Politehnica University of Bucharest, Romania
E-mail: stefan.rosu@upb.ro, conrad_1944@yahoo.com, teodorescu.mihail.stefan@gmail.com
**Politecnico di Torino, Italy
E-mail: **paolo.guglielmi@polito.it, radu.bojoi@polito.it, michele.pastorelli@polito.it**

Abstract–*This paper presents a simple power loss estimation method for inverter-fed low power AC asynchronous and synchronous motors. The method uses a simulation based DC/AC converter power loss estimation based on datasheet parameters and load characteristics like measured phase resistance and current phase delay. A current control scheme is used to impose a constant current at various speeds. Using this approach both asynchronous and synchronous motors can be used as a load. Total power loss is measured as the DC Link current by an amperemeter avoiding the use of complicated measurement systems.*

Keywords: *power loss estimation, PWM parameters, Induction Motor, Synchronous Reluctance, Permanent Magnet Motor.*

1. INTRODUCTION

DC/AC converter driven three-phase motor is becoming the dominant choice in low power industrial, automotive and home appliances systems. More efficient AC machines and optimal control techniques have an important role in system efficiency. While the induction motor (IM) is still a good choice for many applications, the use of synchronous machines like Synchronous Reluctance (SyR) and Permanent Magnet Assisted Synchronous Reluctance (PMASR) can offer higher power density and higher efficiency. Because pulsewidth modulation (PWM) is used to drive the motors, it is important to analyze the PWM converter influence on the system power loss.

Among power electronics devices loss estimation methods are those that assume ideal loads, [1], linear switching energies and analytical formulations [2], or extensive measurement systems [3]. Promising methods use curve fitting of device parameters and simulation waveforms [4]–[6], or measured waveforms [7].

The impact that PWM harmonics have on induction machine was investigated in [8]-[10] concentrating mainly on the additional iron losses. The system power loss was analyzed in [11] by varying the switching frequency.

Losses in permanent magnet motors were investigated in [12] with sinusoidal supply with the help of finite-element method (FEM) and the effect of carrier harmonics of PWM inverter was taken into account in [13], [14].

Previous methods have the advantage of detailed results with separated losses inside the motors but require complicated test setups and FEM analysis. From a system point of view a simple method will suffice to determine the inverter and motor total losses in order to optimize the converter heat sink and other system parameters.

2. PROPOSED METHOD

Considering a simple PWM inverter-fed three-phase motor system like the one in Fig. 1, the total power loss considering no-load condition is

$$P_{tot} = P_{inv} + P_{mot} = V_{dc} * i_{dc} \qquad (1)$$

where P_{inv} is the power loss in the inverter and P_{mot} is the power loss in the motor including mechanical losses.

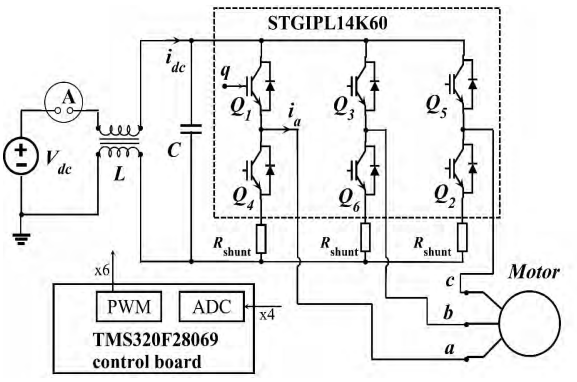

Fig. 1. Schematic of the test circuit

978-1-4673-0738-3/12/$31.00 © 2012 IEEE

Considering a standard DC Link metallized polypropylene film capacitor (MKP) with a small ESR, all the switching ripple current will be contained in the capacitor and the i_{dc} current can be easily measured. A double current choke was used to smooth the current drawn from the DC voltage supply. The power loss of the converter is estimated based on simulation [4], [5], with datasheet parameters curve-fitting, Fig. 2, Fig. 3 and inverter leg operations in Table 1 obtained from the upper IGBT command signal q and phase current sign. A standard Space Vector Modulation (SVM) was used and the phase load currents and reference voltages are shown in Fig. 4. Additional details of the system are provided in Appendix.

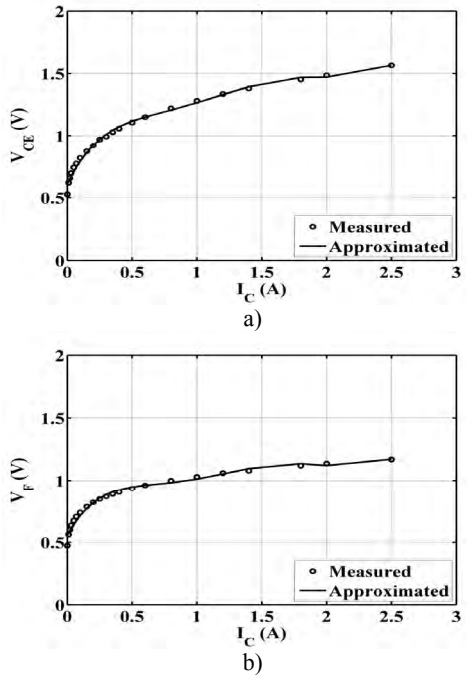

Fig. 2. IGBT and diode ON state voltage.

Table 1. Inverter leg operation

Case	Current	Gate signal of Q_1	Operation
1	$i_a(k) \geq 0$	$q(k\text{-}1)=0$ & $q(k)=0$	D4 conducts
2	$i_a(k) \geq 0$	$q(k\text{-}1)=0$ & $q(k)=1$	D4 turns off Q1 turns on
3	$i_a(k) \geq 0$	$q(k\text{-}1)=1$ & $q(k)=0$	Q1 turns off
4	$i_a(k) \geq 0$	$q(k\text{-}1)=1$ & $q(k)=1$	Q1 conducts
5	$i_a(k) < 0$	$q(k\text{-}1)=0$ & $q(k)=0$	Q4 conducts
6	$i_a(k) < 0$	$q(k\text{-}1)=0$ & $q(k)=1$	Q4 turns off
7	$i_a(k) < 0$	$q(k\text{-}1)=1$ & $q(k)=0$	D1 turns off Q4 turns on
8	$i_a(k) < 0$	$q(k\text{-}1)=1$ & $q(k)=1$	D1 conducts

For low power applications Intelligent Power Modules (IPM) are a common choice but datasheet parameters could be insufficient for an accurate estimation. In this case the on state transistor and diode voltages were measured and curve-fitted with a 5th order polynomial. The switching energy losses were approximated with a 2nd order polynomial based on additional manufacturer data, but they could also be measured. It is worth mentioning that when the lower transistor or diode conducts the power loss of the shunt resistor is taken into account.

The conduction and switching power losses are evaluated every simulation step and averaged every fundamental period [6], [7]. The step size is 100ns, similar to transistor switching times.

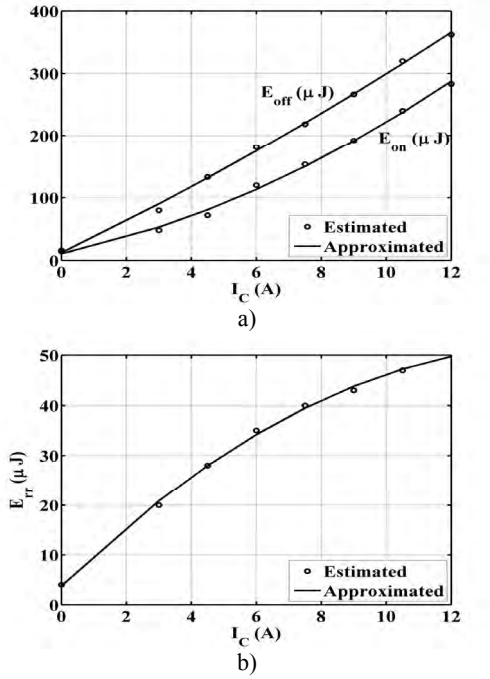

Fig. 3. IGBT and diode estimated switching losses, $V_{dc} = 390V, T_j = 30°C$.

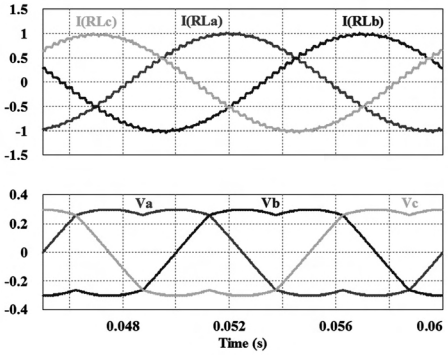

Fig. 4. Load currents (0.5A/div) and SVM phase voltage (0.2p.u./div) reference waveforms.

A RL load was used in the simulations in order to minimize the total simulation time. The resistance is equal to the motor phase resistance and the inductance was calculated to obtain the same current phase delay.

For the motor control, a standard current control scheme implemented in a rotating (*d, q*) frame is used to impose a constant i_d current at various speeds while keeping the i_q current zero, thus generating a rotating magnetic field.

3. RESULTS

The measured total loss is plotted for different switching frequencies and speeds in Fig. 5 b), c), for the IM, in Fig. 6 for the SyR and in Fig. 7 for the PMASR motors. It is worth mentioning that the motors have the same stator frame. The inverter power loss in Fig. 5 a) shows little difference between 0 and 2000 rpm operation. The power loss difference between motors is less than 5% because of small variations in current phase delays. The power loss evolution as the switching frequency increases for the IM is consistent with previous results [8]-[10]. The SyR motor has a smaller variation of the power loss mainly because of lower rotor iron losses. The PMASR motor has a similar rotor structure with the SyR but with additional plastic ferrite magnets. The losses have an increased variation compared to SyR but lower than the IM.

4. CONCLUSIONS

A simple power loss estimation method for inverter-fed motor systems has been presented. The advantage of the method is that it can be applied to synchronous and asynchronous motors with a simple measurement and simulation. Novel comparative results have been presented for the IM, SyR and PMASR motors power loss variation over different switching frequencies.

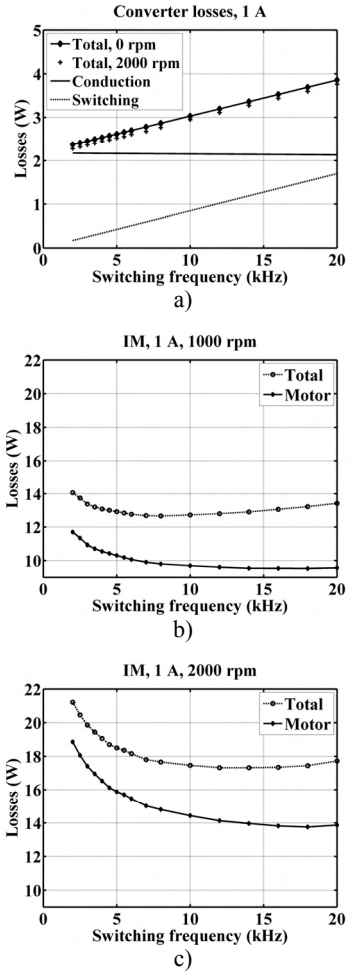

Fig. 5. Losses of the inverter (simulated) and the IM.

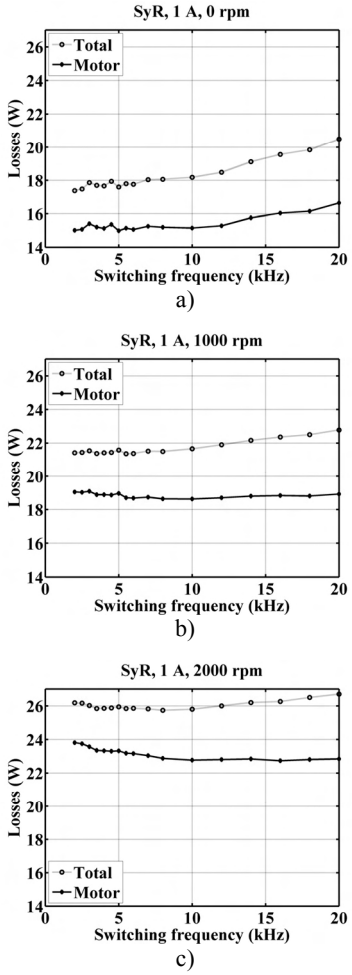

Fig. 6. Losses of the SyR motor.

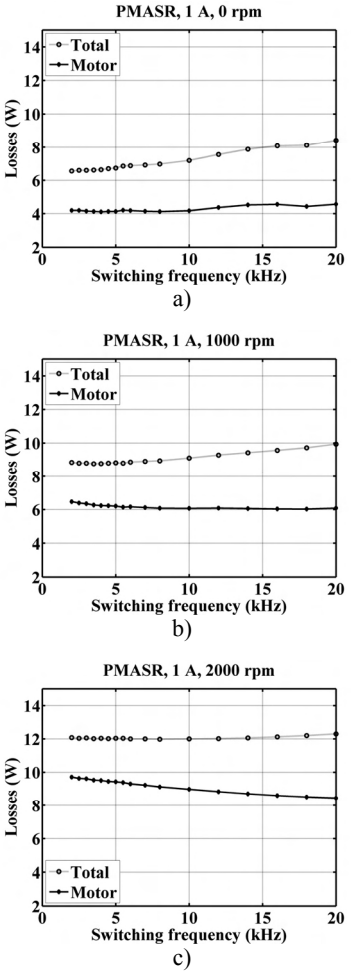

Fig. 7. Losses of the PMASR motor

5. APPENDIX

The experimental tests have been performed with a DC/AC converter prototype based on the ST Microelectronics STGIPL14K60 intelligent power module (IPM) with 1 μs of dead-time. It contains 6 IGBTs and drivers, 3 operational amplifiers for current sensing and 3 comparators for overcurrent protection. The value of the shunt resistor is $0.0375\,\Omega$, the DC Link capacitor C is 35uF and the inductance L is 2x27mH. The schematic of the test circuit is shown in Fig. 1 and a snapshot of the rig in Fig. 8. The inverter DC Link voltage is 200V, supplied by a regulated DC voltage supply. The parameters of the motors are presented in Table 2.

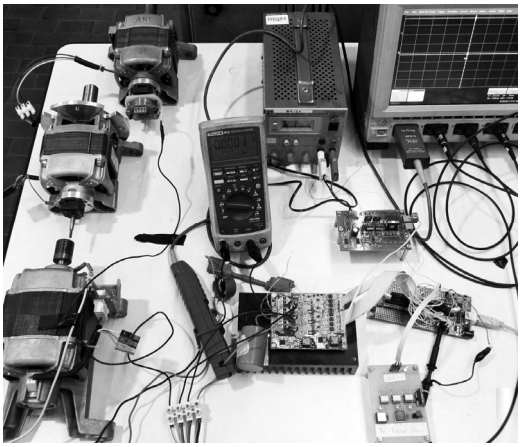

Fig. 8. Test rig. The three motors, from top: PMASR, SyR, IM. The inverter board is in the center.

Table 2. Motor parameters

Parameter	IM	SyR	PMASR
Power (W)	800	400	800
Voltage (V)	195	195	195
Current (A)	3	1.4	3
Max. Speed (rpm)	17000	10000	16000
Nr. of pole pairs	1	2	2
Phase resistance (Ω)	2.8	7.3	1.8
Winding	Cu	Al	Cu
Stack Length (mm)	55	35	40

Acknoledgement–This work was funded by the Sectoral Operational Programme Human Resources Development 2007-2013 of the Romanian Ministry of Labour, Family and Social Protection through the Financial Agreement POSDRU/88/1.5/S/61178.

The authors wish to thank ST Microelectronics support team for providing data regarding switching losses of the IPM.

References

[1] K. Berringer, J. Marvin, and P. Perruchoud, "Semiconductor power losses in AC inverters," *in Proc. IEEE IAS Ann. Meeting*, pp. 882–888, 1995.

[2] F. Blaabjerg, J. K. Pedersen, S. Sigurjonsson, and A. Elkjaer, "An extended model of power losses in hard-switched IGBT-inverters," *in Proc. IEEE IAS Ann. Meeting*, pp. 1454–1463, 1996.

[3] Y. Shen, Y. Xiong, J. Jiang, Y. Deng, X. He, and Z. Zeng, "Switching loss analysis and modeling of power semiconductor devices based on an automatic measurement system," *in Proc. IEEE Int. Symp. Ind. Electron*., pp. 853–858, 2006.

[4] B. Cassimere, S.D. Sudhoff, B. Cassimere, D.C. Aliprantis, and M.D. Swinney, "IGBT and PN junction diode loss modeling for system simulations," *in Proc. Int. Conf. Elect. Mach. Drives*, pp. 941–949, 2005.

[5] R. Mecke, "Multilevel NPC inverter for low-voltage applications," i*n Proc. Eur. Conf. Power Electron. and Appl.*, pp. 1–10, 2011.

[6] A. Sanchez-Ruiz, M. Mazuela, S. Alvarez, G. Abad, and I. Baraia, "Medium Voltage–High Power Converter Topologies Comparison Procedure, for a 6.6 kV Drive Application Using 4.5 kV IGBT Modules," *IEEE Trans. Ind. Electron*., **59**(3), pp. 1462–1476, March 2012.

[7] A.M. Bazzi, P.T. Krein, J.W. Kimball, and K. Kepley, "IGBT and Diode Loss Estimation Under Hysteresis Switching," *IEEE Trans. Power Electron*., **27**(3), pp. 1044–1048, March 2012.

[8] A. Boglietti, P. Ferraris, M. Lazzari, and M. Pastorelli, "Influence of the inverter characteristics on the iron losses in PWM inverter-fed induction motors," *IEEE Trans. Ind. Appl.*, **32**(5), pp. 1190–1194, Sep./Oct. 1996.

[9] A. Boglietti, A. Cavagnino, and A. M. Knight, "Isolating the impact of PWM modulation on motor iron losses," *in Proc. IEEE IAS Ann. Meeting,* pp. 1–7, 2008.

[10] K. Bradley, Cao Wenping, J. Clare, and P. Wheeler, "Predicting Inverter-Induced Harmonic Loss by Improved Harmonic Injection," *IEEE Trans. Power Electron*., **23**(5), pp. 2619–2624, Sep. 2008.

[11] J.R. Wells, B.M. Nee, P.L. Chapman, and P. T. Krein, "Optimal harmonic elimination control," *in Proc. IEEE Power Electronics Specialists Conf*., pp. 4214–4219, 2004.

[12] O. Bottauscio, G. Pellegrino, P. Guglielmi, M. Chiampi, and A. Vagati, "Rotor loss estimation in permanent magnet machines with concentrated windings," *IEEE Trans. Magn*., **41**(10), pp. 3913–3915, Oct. 2005.

[13] K. Yamazaki and S. Watari, "Loss analysis of permanent-magnet motor considering carrier harmonics of PWM inverter using combination of 2-D and 3-D finite-element method," *IEEE Trans. Magn*., **41**(5), pp. 1980–1983, May 2005.

[14] K. Yamazaki and A. Abe, "Loss Investigation of Interior Permanent-Magnet Motors Considering Carrier Harmonics and Magnet Eddy Currents," *IEEE Trans. Ind. Appl*., **45**(2), pp. 659–665, March/April 2009.